

**KERNFORSCHUNGSZENTRUM  
KARLSRUHE**

November 1969

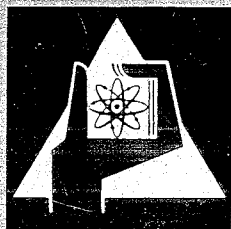
KFK 1088

Institut für Angewandte Reaktorphysik

The Saturn Code

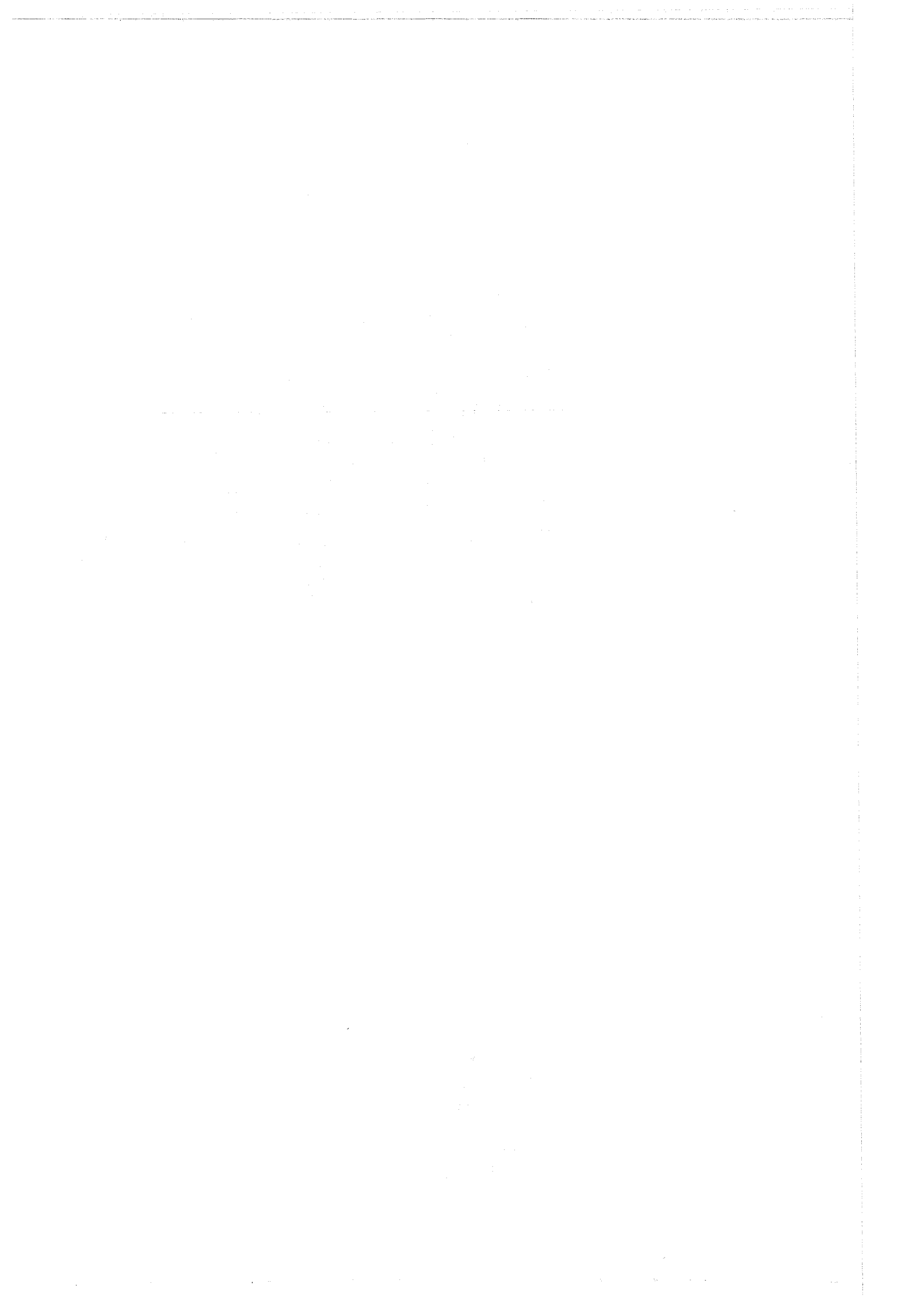
A Theoretical Analysis of Fuel Pin Behavior and Fuel Void Dynamics

H. Kämpf, G. Karsten



GESELLSCHAFT FÜR KERNFORSCHUNG M. B. H.

KARLSRUHE



KERNFORSCHUNGSZENTRUM KARLSRUHE

November 1969

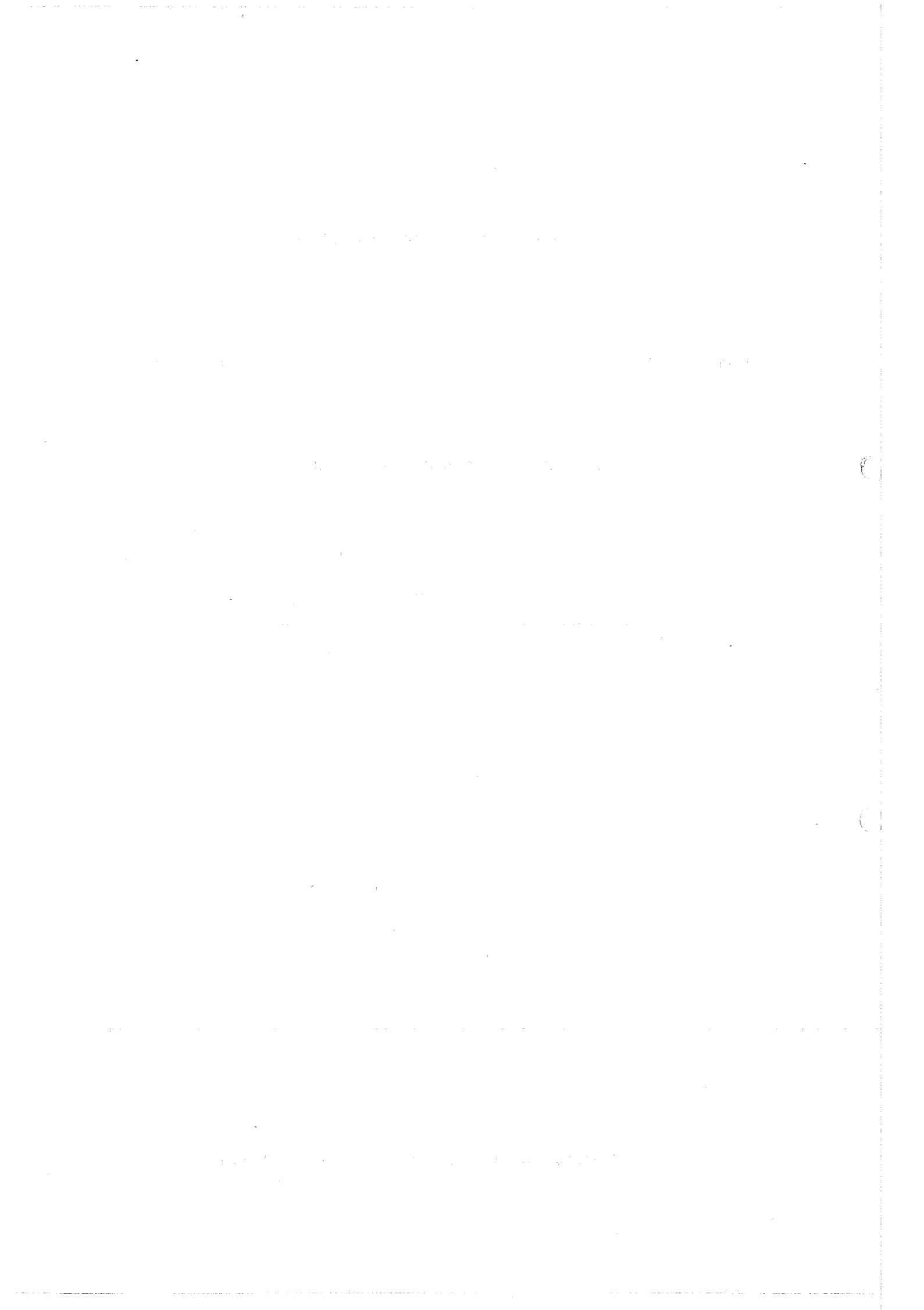
KFK 1088

Institut für Angewandte Reaktorphysik

The Saturn Code  
A Theoretical Analysis of Fuel Pin Behavior  
and Fuel Void Dynamics

H. Kämpf, G. Karsten

Gesellschaft für Kernforschung mbH, Karlsruhe



## Abstract

The SATURN - Code, swell and thermal analysis under reactor conditions, contains a macroscopic modelling analysis of the thermal and mechanical effects of the different types of void volumes. This paper follows a presentation given on the ANS - winter meeting 1968 and published in KFK 878 "Theoretical and Computer Analysis on the Behavior of Fast Reactor Fuel Pins and Related Parts of the Core Under Operational Conditions". Its basis was an application of the original form of the SATURN - Code on a core analysis; a graph of a core analysis is given in this paper in fig. 13.

The first part of this paper treats the thermal effects of the porosity, central void and open gas gap. A new relation for the porosity dependence of the thermal conductivity is deduced. For given gas contents and determined ranges of pore temperatures and sizes a simple approximate equation results. Central void is very effective in reducing the central temperature; making use of it means increasing the linear rod power. The in-pile migration of the porosity in the hotter regions of oxide fuel forms resp. increases the central void and densifies the hotter region. This effect is calculated by a two - zone porosity model. For the open ideal gap fuel - clad filled with inert gases and mixtures of He with fission product gas mixtures the temperature drop is calculated as a function of gap width, linear rod power, clad inside temperature and clad inside radius.

The second part of this paper treats the interaction and burnup behavior. The problem is partitioned concerning weak and strong contact interaction. The weak contact interaction is realized if cracks caused by thermal expansion are existent. A way is described to treat the gas - swelling and the stress strain state of the swelling crack -free fuel in contact with the clad. For the case of a hollow cylindrical fuel a two-zone model consisting of the fuel and the clad is used with a strong axial friction force in the interface . For the solid cylindrical fuel a three - zone model consisting of two fuel zones is proposed. While a strong axial friction force is assumed between the outer fuel zone and the clad, this friction force is neglected between the two fuel zones.



## C o n t e n t s

1. Introduction
2. Thermal behavior
  - 2.1 Porosity effect on thermal conductivity
  - 2.2 Thermal central void effect and in-pile pore migration
  - 2.3 Thermal gap effect
3. Interaction and burnup behavior
  - 3.1 Weak contact interaction during "the crack phase"
  - 3.2 Strong contact interaction of a solid or hollow cylindrical fuel  
with the clad



## 1. Introduction

This paper deals with a macroscopic modelling analysis of the thermal and mechanical effects of the different types of internal void volumes such as open and closed porosity central void, open and closed gap, crack structure, dishing and radial wedges, and their changes under operation. This analysis is based on the fact that fuel swelling is at present the most important effect in regard to the burnup limitation. Therefore the type, size and shape of internal void resp. gas volumes, and their in pile changes are of great importance for the fuel pin design.

All these equations and models are compiled in the SATURN - code, swell and thermal analysis under reactor conditions. In a more completed and elaborated stage this code is intended to calculate pin designs and operational pin behavior especially in view of the German SNR core. This code will not claim to make exact predictions of pin behaviour; it is thought to be a selective tool and help for economy in core designs.

## 2. Thermal behavior

The first part of the work treats the thermal effects caused by the different types of void volumes especially by the porosity, the central void and the open gap fuel clad.

### 2.1 Porosity effect on thermal conductivity

There is a considerable divergency between the existing theoretical relations for the porosity dependence of the thermal conductivity and the known experimental data as is shown later in the discussion of our results. The relationship based on the following model is in a satisfactory agreement with the results experimentally obtained. If the real porosity structures according to fig 1. are idealized by arrangements on the base of connecting in parallel and in series of the fully dense and the void volumes, it is possible to calculate the thermal conductivities of any porous body such as sintered material with an anisotropic pore distribution or powder material. The practical applicability often fails because necessary input data as e.g. the open and closed porosity and the degree of anisotropy are not known.

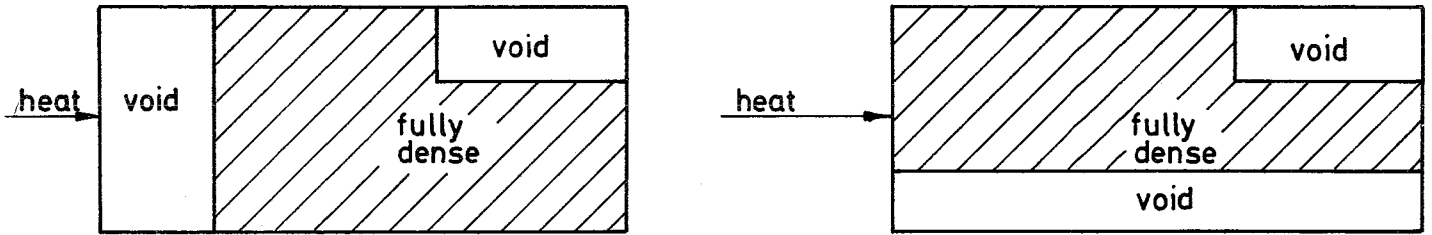


Fig. 1 Possible models for the arrangements of the fully dense and the porous phase.

In the appendix A the simpler case of isolated resp. closed porosity is calculated according to the following model:

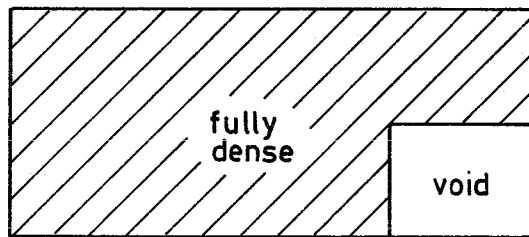


Fig. 2 Model for a sintered body with only closed porosity.

The following general relationship for the porosity dependence of the thermal conductivity is obtained

$$k = k_o \left[ 1 - aP^{2/3} \left( 1 - \frac{1}{1 + \frac{1}{a} P^{1/3} (\kappa - 1)} \right) \right] \quad (1)$$

- where
- $k$  = thermal conductivity of the porous material
  - $k_o$  = thermal conductivity of the fully dense material
  - $\kappa = \frac{k_o}{k_p}$  ratio of  $k_o$  to  $k_p$ .  $k_p$  is the thermal conductivity of the pore
  - $P$  = porosity = relative volume fraction of the pore phase
  - $a$  = anisotropy factor ( $a = 1$  means isotropic pore distribution)

This relationship is of course not only valid for a porous fuel but generally for any two-phase system such as e.g. for cerments. We realize that the anisotropy factor  $a$  and the ratio  $\kappa$  of the thermal conductivity  $k_o$  to  $k_p$  are characteristic of this relationship.

It has to be noted that isotropy is related to a statistically averaged macroscopic region; locally anisotropic pore shapes are allowed.

For the critical case given by  $\kappa \rightarrow \infty$  and isotropic pore distribution  $a = 1$ , which is very important in practice, the following approximate equation results from equation (1)

$$k = k_o (1 - P^{2/3}) \quad (2)$$

In fig. 3 the ratio of the thermal conductivity of the porous material  $k$  to the thermal conductivity of the fully dense material  $k_o$  is plotted versus the porosity for the special case of isotropic pore distribution given by  $a = 1$  with  $\kappa$  as parameter. The thick line represents the critical case for  $\kappa \rightarrow \infty$  given by equation (2), which is a good approximation for  $\kappa$  values greater than 50.

As the linear dependences

$$\frac{k}{k_o} = 1 - \eta P \quad (3)$$

are sometimes used in literature, the curve  $1 - P^{2/3}$  is replaced by straight lines in three successive porosity ranges. The slopes  $\eta$  of this straight lines have the following values:

For	$0 \leq P \leq 0.1$	$\eta = 2.5$	
	$0.1 \leq P \leq 0.15$	$\eta = 2$	(4)
	$0.15 \leq P \leq 0.25$	$\eta = 1.7$	

The strong decrease of the thermal conductivity at small porosities is especially remarkable. The relative decrease of the thermal conductivity becomes smaller with increasing porosity.

The ratio  $\kappa = \frac{k_o}{k_p}$  of the thermal conductivity of the fully dense material  $k_o$  to the thermal conductivity of the pores  $k_p$  has to be calculated to evaluate numerically relation (1) and to realize under which conditions the approximate relation (2) is valid. In treating the heat transfer through the open ideal gap in chapter 2.3 the following equation for the thermal conductivity of the uni-dimensional gap  $k_p$  is deduced.

$$k_P = \underbrace{k_C T_P^s}_{\text{part of conduction}} + \underbrace{4C_R T_P^3 \delta}_{\text{part of radiation}} \quad (5)$$

where

- $T_P$  = (absolute) temperature within the pore
- $\delta$  = gap width
- $k_C T_P^s$  = thermal conductivity of the filling gas.  $k_C$  and  $s$  are gas properties
- $C_R$  = material properties related to the coefficient of emissivity

Equation (5) can directly be applied for the cracks oriented perpendicularly to heat flow direction and for the cylindrical pores with axes parallel to heat flow direction. For pores which are spherical and cylindrical with axes perpendicular to heat flow direction the introduction of a shape factor  $\psi$  is necessary. Thus one gets.

$$k_P = k_C T_P^s + 4C_R T_P^3 \psi d \quad (6)$$

where

- $\psi$  = shape factor
- $d$  = largest dimension of pore in direction of heat flow

The following values are deduced in the appendix B

$$\begin{aligned} \psi &= \frac{\pi}{4} = 0.79 && \text{for spherical pores} \\ \psi &= \frac{2}{\pi} = 0.64 && \text{for cylindrical pores with axis perpendicular} \\ &&& \text{to heat flow direction} \end{aligned}$$

The shape of the pores has only a weak influence on the heat conductivity of the pores. For the case of isotropic pore distribution statistically averaged over a macroscopic region, the anisotropic pore shapes have to compensate. According to equation (6) the thermal conductivity of the pore strongly depends on the temperature in the radiation part, furthermore it is proportional to the pore dimension.

In fig. 4 the ratio  $\kappa = k_o/k_p$  for oxide is plotted versus the pore dimension, pore temperature and type of gas are parameters. The maximum temperature of interest is about 1700°C on account of the pore migration towards the center of the fuel for higher temperatures. It can be seen that for He  $\kappa$  ratios are only weakly dependent on pore dimension as in this case the part of radiation is negligible. It is required to apply the lengthy expression (1) because  $\kappa$  values about 5 result. The influence of the pore dimension is considerable for fission product gas consisting of 15 % Kr and 85 % Xe as in this case the part of the radiation is of the same order as the part of the conduction. The approximate equation (2) can be applied for pore sizes up to 100  $\mu$  and more at a temperature about 1000°C and for pore sizes smaller than about 30  $\mu$  at temperatures about 1700°C. As the thermal conductivities for carbide are about 7 times greater than for oxide, these  $\kappa$  values have to be multiplied by a factor about 7. Therefore the approximate equation (2) is valid for carbide in a wide range.

By differentiating equation (2) it can be seen that the relative conductivity change due to an absolute change of the porosity resp. of the relative fuel density is constant over a wide range of density. The following relation results

$$\text{for } 0.70 \leq D_F \leq 0.92 \quad \frac{\Delta k}{k} = 1.75 \Delta D_F \quad (7)$$

$$D_F = 1 - P = \text{relative fuel density}$$

Two practically important consequences result from equation (7)

$$\text{a. } \chi = \text{const.} \quad \frac{\Delta(T_o - T_F)}{T_o - T_F} = - 1.75 \Delta D_F \quad (8)$$

$$\text{b. } T_o, T_C = \text{const.} \quad \frac{\Delta \chi}{\chi} = 1.75 \frac{T_o - T_F}{T_o - T_C} \Delta D_F \quad (9)$$

where

- $\chi$  = linear rod power
- $T_o$  = central temperature
- $T_F$  = fuel surface temperature
- $T_C$  = coolant temperature

That means:

- a. An absolute density change of 10 % causes a relative change of the temperature drop in the fuel of 17.5 %.
- b. The temperature ratio  $(T_o - T_F)/T_o - T_C$  is about 1 for oxide and carbide with Na-bonding, for carbide with He-bonding about 1/2. Therefore an absolute density change of 10 % causes a relative change of linear rod power of 17.5 % resp. about 9 %.

These results, especially the strong decrease of the thermal conductivity at small porosities are in a good agreement with experimentally obtained results <1 to 6>. In a report <7> published recently a still stronger decrease compared with that of fig. 3 was obtained, furthermore the porosity dependence was obtained as temperature dependent. These results are in accordance with ours if a temperature dependent anisotropy of the porosity distribution is assumed. In literature some theoretical relationships are known the most prominent of which are the simplified form of the Loeb equation <8>, the Maxwell - Eucken equation <9>.

$$\frac{k}{k_o} = 1 - P \langle 8 \rangle \quad \text{resp.} \quad \frac{k}{k_o} = \frac{1 - P}{1 + \frac{P}{2}} \langle 9 \rangle$$

and the equation of Russell <10>. All these equations supply a too small almost linear decrease of the thermal conductivity. Better agreements could only be reached by the introduction of fitting factors. A theoretical treatment of recent date <11,12> led to an opposite trend of the factors  $\eta$  compared with the values of (4) i.e. increasing values of  $\eta$  for increasing porosities.

## 2.2 Thermal central void effect and in-pile pore migration

By the fabrication of a central void the most effective possibility is given to reduce the temperature distribution in order to increase the linear rod power. For oxide fuel an in-pile pore migration towards the center of the fuel occurs in hot fuel regions for temperatures above ca. 1700°C. This pore migration causes a formation or an increase of the central void and a densification of this hotter fuel region. Both effects lead to a possible increase of the linear rod power for a given central temperature. In <13> this effect was calculated by a three-zone model. But with regard to the relatively small zone of the porosity change the application of a two-zone porosity model is

reasonable. In <14,15> the increase of the linear rod power was calculated with a two-zone model but without regarding the densification effect and by fixing the fuel surface and center temperature. As by a change of linear rod power the relative large temperature drop in the gap fuel-clad also changes, it is more realistic to fix coolant or clad temperature and the central temperature. In <16> we generally treated the two-zone model. Especially the densification was considered by the  $(1 - P^{2/3})$  - relation. On account of completeness a summary is given in appendix C. The following equations for the temperature drops in the two porosity zones are obtained:

$$\int_{T_P}^{T_O} k_o(T) dT = \frac{\chi}{4\pi D_o} \cdot \frac{1 - P_I}{1 - P_I^{2/3}} \left[ \left( \frac{r_P}{r_F} \right)^2 - \left( \frac{r_o}{r_F} \right)^2 - \left( \frac{r_o}{r_F} \right)^2 \ln \left( \frac{r_P}{r_o} \right)^2 \right] \quad (10)$$

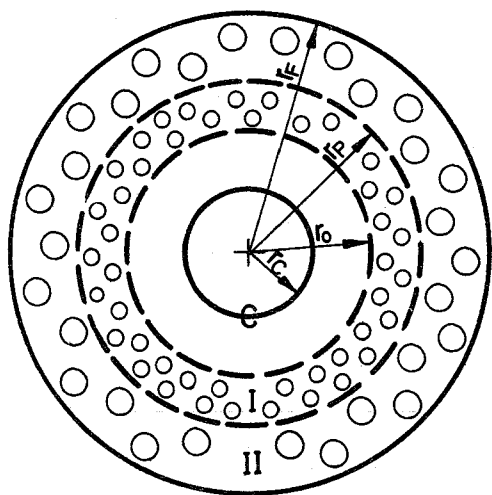
$$\int_{T_F}^{T_P} k_o(T) dT = \frac{\chi}{4\pi D_o} \cdot \frac{1 - P_{II}}{1 - P_{II}^{2/3}} \left[ 1 - \left( \frac{r_P}{r_F} \right)^2 - \left( \frac{D_o}{1 - P_{II}} - 1 \right) \ln \left( \frac{r_F}{r_P} \right)^2 \right] \quad (11)$$

- $k_o$  = thermal conductivity of the fully dense material
- $\chi$  = linear rod power
- $D_o$  = relative fuel density for a reference solid or hollow cylinder of homogenous porosity distribution with the same linear rod power and fuel radius. In the case of a hollow cylinder  $D_o$  means the smear density relating to the fuel radius.

The other symbols are explained in the next figure.

Two assumptions relating to the amount of migrating porosity on the base of a two - zone model are possible. The porosity above a given temperature related to the pellet density or related to the smear density migrate to the center. The last assumption is probably realistic for large fabricated gap widths because of gap closure during startup (chapter 2.3). Correspondingly the porosity of the outer zone related to pellet density or to the smear density remains unchanged.

In the following only the case of porosity migration related to the pellet density is calculated according to figure 5.



- C = central void
- I = inner densified zone with porosity  $P_I$
- II = outer zone of unchanged fabricated porosity  $P_{II}$
- $r_C$  = fabricated central void radius
- $r_o$  = central void radius after porosity migration
- $r_P$  = zone boundary radius
- $r_F$  = fuel radius
- $T_o = T(r_o)$      $T_P = T(r_P)$      $T_F = T(r_F)$

Fig. 5 Two-zone porosity model for the porosity migration in a hollow cylinder of homogenous fabricated porosity.

From a mass balance the following relations between the porosities and the radii are obtained

$$D_o = (1 - P_{II}) \left[ 1 - \left( \frac{r_C}{r_F} \right)^2 \right] \quad (12)$$

$$r_o^2 = \frac{1 - P_{II}}{1 - P_I} r_C^2 + \frac{P_{II} - P_I}{1 - P_I} r_P^2 \quad (13)$$

For the numerical evaluation the following temperature dependence of the thermal conductivity for the fully dense stoichiometric  $UO_2$  resp.  $(U_{0.8}Pu_{0.2})O_2$  is used.

$$k_o(T) = \frac{41.2}{T + 4.9} + 6.55 \cdot 10^{-13} T^3 \left[ \frac{W}{cm^{\circ}C} \right] \quad T \text{ in } ^{\circ}K \quad (14)$$

This equation was obtained by averaging the results of the following authors <17 to 22> and by using the  $(1 - p^{2/3})$ -relation.

In fig. 6 the linear rod power is plotted versus the relative fabricated central void volume for homogenous porosity distribution and for the two-zone model caused by the porosity migration. Central temperature and clad inner

temperature are fixed, smear density is parameter. It can be seen that for homogenous porosity distribution a steep increase of the linear rod power occurs by increasing the fabricated central void volume. Increasing the smear density leads roughly to a parallel shift of the curves in direction to higher linear rod powers because of the better thermal conductivity in the hollow cylinder. Considering the pore migration by using the two-zone porosity model, the linear rod powers are considerably higher especially for small fabricated void volumes. It must be noticed that the real central void volumes are larger especially for small void volumes and low smear densities. For relatively small fabricated central void volumes the linear rod power is higher at low smear densities because of the dominant increase of the in pile central void. For large fabricated central void volumes the linear rod powers trend to increase with enlarging smear densities because of the dominant increase of the thermal conductivity.

In fig. 7 the linear rod power of a hollow cylinder related to that of a solid cylinder of the same smear density is plotted versus the relative central void volume for oxide and for carbide with He- and Na-bonding according to:

$$\frac{x_H}{x_S} = \frac{\frac{r_F \cdot h}{2\bar{k}_o \left[ 1 - (1 - D_o)^{2/3} \right] + 1}}{\frac{r_F \cdot h \left[ 1 - \frac{1}{(r_F/r_o)^2 - 1} \ln (r_F/r_o)^2 \right]}{2\bar{k}_o \left[ 1 - \left( 1 - \frac{D_o}{(1 - r_o/r_F)^2} \right)^{2/3} \right]}} \quad (15)$$

- $\frac{x_H}{x_S}$  = ratio of the linear rod power of the hollow cylinder to that of the solid cylinder
- h = heat transfer coefficient fuel-clad
- $k_o$  = thermal conductivity of the fully dense fuel (temperature averaged)

This relation is deduced in Appendix C. A homogenous porosity distribution is assumed, furthermore the central temperature and clad inner temperature are fixed. These ratios of the linear rod powers are nearly independent of the smear density. Of course the linear rod powers themselves become smaller with decreasing smear density because of the decreasing thermal conductivity. The increase of the linear rod power for carbide with He-bonding is roughly less than half of that of oxide, the increase of the linear rod power for carbide with Na-bonding is a little more than that of oxide.

### 2.3 Thermal effect of the gap fuel clad

Two cases have to be discerned concerning the mean free path of the gas molecules which can be larger or smaller than the gap width. Under operating conditions the mean free path for all gases is smaller than  $1 \mu$ . That means that the case for which the mean free path is larger than the gap width can only be realized for the contact of the fuel and the clad by the roughness of the surfaces. In the following only the case of the open gap is treated. This case is of great importance for the mechanism of the gap closure and opening during thermal cycling e.g. during the startup phase.

In <23> we treated this case which is brought up to date. In the appendix D the following equation for the temperature drop in the open ideal gap is obtained:

$$\delta = \frac{C_C T_I^{s+1} \left[ \left( 1 + \frac{\Delta T}{T_I} \right)^{s+1} - 1 \right]}{\frac{\chi}{2\pi r_I} - C_R T_I^4 \left[ \left( 1 + \frac{\Delta T}{T_I} \right)^4 - 1 \right]} \quad (16)$$

- $\delta$  = gap width, constant along the fuel surface
- $\Delta T$  = temperature drop in the gap
- $T_I$  = internal clad temperature
- $r_I$  = internal clad radius
- $\chi$  = linear rod power

with

$$C_C = \frac{k_C}{s + 1} \quad (17)$$

$k_C, s$  = gas constants related to the thermal conductivity of the gas contents according to equation (19)

and

$$C_R = \frac{\sigma}{\frac{1}{\epsilon_1} + \frac{1}{\epsilon_2} - 1} \quad (18)$$

- $\sigma$  = Stefan Boltzmann constant
- $\epsilon_{1,2}$  = emissivities of the fuel - resp. the internal clad surface

The following equation experimentally obtained <24> was used for the thermal conductivity of the possible gases, i.e. of filling gases He and Ar and of the fission product gas mixtures of Kr and Xe

$$k_i = k_{iC} T^s \quad (19)$$

$k_i$  = thermal conductivity with i standing for the gas component i

It has to be noted that the kinetic theory of gases, it is true, supplies principal dependences but the conductivities themselves are relatively inaccurate, so that it is reasonable to use experimentally obtained values. The thermal conductivities in <24> differ a little in the exponent s of the equation (19). In order to describe the different gas types by different  $\delta$  scales in the fig. 8 and 9 we used a mean value of s and adapted the new dependence to 800°K. The resulting error is smaller than 5 %, which is within the inaccuracy of these values. Table 1 contains the so obtained thermal conductivities.

Table 1: Thermal conductivities of the inert gases

gas type	thermal conductivity k $\left[ \frac{W}{cm^{\circ}C} \right]$
He	$k = \left\{ \begin{array}{l} 1.58 \cdot 10^{-5} \\ 1.97 \cdot 10^{-6} \\ 1.15 \cdot 10^{-6} \\ 0.72 \cdot 10^{-6} \end{array} \right\} T^{0.79}$
Ar	
Kr	
Xe	

T in abs. temp. °K

The following experimental result concerning the thermal conductivities of gas mixtures is reported in <24,25>. If the volumetric concentration is plotted along a linear scale and the conductivity along a logarithmic scale nearly straight lines result. That means the following concentration dependence of the thermal conductivity is approximately valid.

$$k = k_1^{x_1} \cdot k_2^{x_2} \quad \text{with } x_1 + x_2 = 1 \quad (20)$$

- $k_{1,2}$  = thermal conductivities of the pure components 1 and 2  
 $x_{1,2}$  = volumetric concentration of the two components

The following simple expression for the concentration and temperature dependence of the thermal conductivity of a binary mixture is got by putting equation (19) into equation (20).

$$k = k_{1C}^{x_1} \cdot k_{2C}^{x_2} T^s \quad (21)$$

In the same way the thermal conductivities of ternary mixtures e.g. for He and the fission product gas consisting of 15 % Kr and 85 % Xe can be obtained.

In fig. 8 the temperature drop in the open ideal gap is plotted versus the gap width with clad inside temperature, linear rod power and gas type as parameter. Different gap width scales are valid for the gas types such as the inert gases and mixtures with gaseous fission products. For the assumed conditions it can be seen that by increasing the gap width first a steep temperature drop occurs succeeded by a saturation behavior. While the steep increase is given by the prevailing of the conduction part, the saturation phase is given by the prevailing of the radiation part. The temperature drops for the given conditions are relatively large for He. The same temperature drops are reached for the other inert gases and mixtures with the gaseous fission products at remarkably smaller gap widths according to the remarkably lower thermal conductivities of these gases.

In fig. 9 the heat transfer coefficient for the open ideal gap is plotted versus the gap width in a double logarithmic plot for the same conditions as in the preceding fig. 8. These curves are obtained simply by the values of fig. 8. It can be seen that for relatively small gap widths straight lines result. The reason for it is that the following equation for the heat transfer coefficient  $h$  for the critical case  $\Delta T \ll T_I$  is valid as it is shown in appendix D.

$$h = k_C T_I^s \frac{1}{\delta} + 4C_R T_I^3 \quad (22)$$

This equation is identical to equation (5). For rather small gap width the second term in (22) is also negligible leading to the straight lines in the double logarithmic graph. For larger gap widths the curves branch out although the influence of clad inside temperature and linear rod power is not very great.

### 3. Interaction and burnup behavior

The treatment of the mechanical, interaction, and burnup behavior of fuel pins, which is underway, starts from the Crash computer program, creep analysis in a fuel pin sheath, for the cladding <26>. This program generally calculates triaxial states of stresses and strains at any time during the lifetime of the creeping cladding for the main assumptions of axisymmetry and plane strain. The input data resp. time dependent input functions are the inner and outer pressure, possibly an additional axial force, the temperature distribution with the thermal expansion, and the creep law. The calculation method consists in the solution of the equilibrium equation, the compatibility equation for the total strains, and the stress strain relations starting from a given state of permanent strains. The total strains are divided in the elastic strains, given by the tridimensional Hookes law, the thermal strains, and the space and time dependent permanent strains. The integration of the equations of this stress strain Problem supplies three integration constants to be determined by three boundary conditions. The calculation is carried out by the following iteration procedure. Starting from a first guess of the permanent strains for a given time interval, the state of stress compatibel with the input functions and the given permanent strains is calculated. By the aid of the given creep law and the Mises or Tresca theory corrected values for the permanent strains are obtained. This procedure is repeated until the convergence is reached and then repeated again for the successive time steps. Basing on the assumptions of axisymmetry and plane strain, the main equations for the stress and strain state of the swelling porous fuel in a temperature field are.

$$\frac{d\sigma_r}{dr} + \frac{\sigma_r - \sigma_\theta}{r} = 0 \quad (23)$$

$\sigma_{r,\theta,z}$  = radial, tangential, resp. axial stress  
 $r$  = radius within the cladding

The relations between the strains and the radial displacement are

$$\epsilon_r = \frac{du}{dr} \quad \epsilon_\theta = \frac{u}{r} \quad \epsilon_z = \text{const.} \quad (24)$$

$\epsilon_{r,\theta,Z}$  = radial, tangential, resp. axial strain

$u$  = radial displacement

and the stress strain relations are

$$\begin{aligned} \epsilon_r &= \frac{1}{E} \left[ \sigma_r - \mu(\sigma_\theta + \sigma_Z) \right] + \alpha T + \beta A + \epsilon_{rc} \\ \epsilon_\theta &= \frac{1}{E} \left[ \sigma_\theta - \mu(\sigma_r + \sigma_Z) \right] + \alpha T + \beta A + \epsilon_{\theta c} \\ \epsilon_Z &= \frac{1}{E} \left[ \sigma_Z - \mu(\sigma_r + \sigma_\theta) \right] + \alpha T + \beta A + \epsilon_{Zc} \end{aligned} \quad (25)$$

$\uparrow$  total                       $\uparrow$  elastic                       $\uparrow$  thermal                       $\uparrow$  swelling                       $\uparrow$  permanent  
 strains

with

$E$  = Young's modulus

$\mu$  = Poisson's ratio

$\alpha$  = thermal expansion coefficient

$T$  = temperature

$\beta$  = (linear) swelling rate

$A$  = burnup

$\epsilon_{ic}$  = ( $i = r,\theta,Z$ ) = radial, tangential, resp. axial permanent strain

The boundary conditions necessary for the solution of the stress and strain state lead, as is shown below, to a partition of the problem.

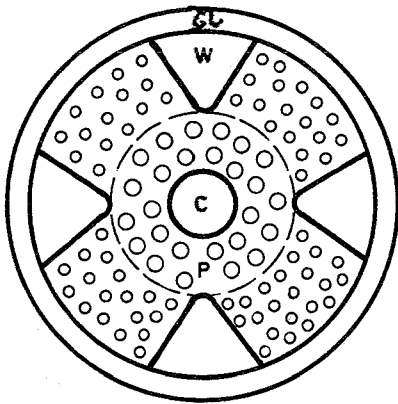
The mechanical behavior of the fuel is much more complicated than that of the clad because of the following main reasons: Firstly, the fuel has a fabricated porosity partly open and partly closed and furthermore develops a porosity filled by fission gas during burnup, the so-called gas swelling. This partly consumes the fabricated porosity. This is corresponding to a relatively large fictive compressibility.. Secondly, the fuel, especially oxide, is brittle for lower temperatures so that cracking occurs where a tensile stress exists e.g. during the thermal cycling. Thirdly, the thermal strain  $\alpha T$  and the swelling strain  $\beta A$  are quite different deformations in regard to their strain rate. While the thermal expansion occurs rather quickly linked with a crack formation, especially for oxide, the swelling expansion occurs long-term. Because of these quite different strain rates connected with a different mecha-

nical behavior it is reasonable to eliminate in (25) the thermal strain  $\alpha T$  in order to treat it separately. This procedure is also reasonable in view of the different interaction behavior characterized by different boundary conditions.

### 3.1 Weak contact interaction during the "crack phase"

A qualitative characterization supplies the following picture. The cracks in oxide are caused by thermal cycling e.g. for the startup phase because of its brittleness for lower temperatures. The thermal expansion is generally given by the brittle-plastic behavior of the fuel, the thermal expansion coefficients of the fuel and the clad, initial gap widths and further void volumes, and the restraining conditions. At the initial time of the startup phase, the fuel forms cracks extending to the central axis of the pin  $\langle 27 \rangle$ . Unrestrained extension occurs in radial and axial direction till the expansion is limited by a restraint in any direction. Then the expansion preferably occurs in direction to the plastic center zone by closing the cracks and partly consuming the porosity in the plastic zone  $\langle 28, 29 \rangle$ . Pellet end-face dishing can be consumed by axial expansion. The porosity in the plastic zone is available in accordance with the gas pressure within the pore, the surface tension pressure, and the restraining outer pressure. In the case of sufficient large initial gap widths the thermal expansion occurs without appreciable contact pressure, a part of the gap volume being localized as crack volume. The succeeding fuel swelling occurs unrestrained in at least one direction, the remaining gap volume being filled without strong contact pressure. The duration of this phase increases with initial gap width which is limited by the thermal gap effect treated in chapter 2.3 .

The duration of the phase of weak contact interaction can be elongated by fabricating radial wedges  $\langle 30 \rangle$  according to fig. 10. For this wedge shaped pellet the tangential swelling in the outer fuel zone with the inferior creep behavior occurs unrestrained in the direction to the wedge shaped void volumes. The radial swelling preferably occurs in the direction to the void volumes of the inner fuel zones, given e.g. by the central void and the porosity because of the superior creep behavior of the central zone. Of course this concept is only effective if the unrestrained low temperature swelling is not considerable larger than the restrained swelling. This concept could become important for He-bonded carbide fuel elements in view of the stronger interaction behavior.



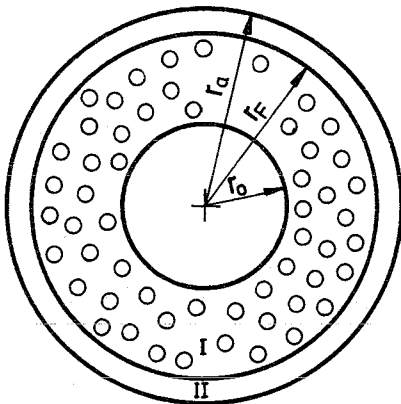
- C = central void
- P = wedge shaped pellet  
(possibly two porosity zones)
- W = wedges
- Cl = cladding

Fig. 10. Pellet with radial wedges causing weak contact interaction during the swelling.

### 3.2 Strong contact interaction of a solid or hollow cylindrical fuel with the clad

After the filling of the gap and crack volumes a contact fuel-cladding is realized. Two cases have to be distinguished concerning the hollow cylindrical fuel resp. solid cylindrical fuel.

For the case of a hollow cylindrical fuel produced by fabrication or by in-pile central void formation the application of a two-zone-model is reasonable.



- I = F fuel zone
- II = Cl cladding
- $r_0$  = central void radius
- $r_F$  = fuel outside radius
- $r_a$  = clad outside radius

Fig. 11 Two-zone model for the case of a hollow cylindrical fuel

The stress strain relations of the clad are given by the equations (25) without the swelling term, the concerning relations for the fuel are given without the thermal strains. On the basis of these equations and the boundary conditions discussed below, the stress and strain state in the fuel and the clad

is determined for a given swelling rate and creep law. The complication arises from the fact that the gas swelling rate itself is stress dependent. Therefore the problem has to be solved by an iteration procedure. Starting from a swelling rate e.g. for the solid fission products, the stresses in the fuel are calculated. These stresses supply a gas swelling rate with the aid of the assumptions below. This procedure is repeated until the convergence is reached. Assumptions concerning the gas swelling are  $\langle 31, 32, 33, 34 \rangle$ .

- a. Not released fission gas forms partly fission gas induced bubbles and partly migrates to fabricated porosity.
- b. A definite distribution of fission gas induced bubbles and fabricated pores is realized and determines the amount of fission gas, per bubble or pore, contributed by a definite fuel volume.
- c. The fission gas bubble radius is determined by the following equilibrium equation.

$$P_f = \frac{2\gamma}{r} + \sigma_H \quad (26)$$

$P_f$  = fission gas pressure within the bubble

$\gamma$  = surface tension of the fuel material

$r$  = radius of bubble

$\sigma_H$  = hydrostatic stress component adjacent to the bubble

The closure of the fabricated porosity is finished if this equilibrium is reached.

The solution of this problem requires the determination of six integration constants given by the boundary conditions. The formulation is trivial for the following four boundary conditions.

- a. The radial stress at the outer surface of the clad is equal to the outer coolant pressure.
- b. The radial stress at the inner surface of the fuel is equal to the inner gas pressure.
- c. The radial stress at the outer surface of the fuel is equal to the radial stress at the inner surface of the clad.
- d. The radial displacement at the outer surface of the fuel is equal to the radial displacement at the inner surface of the clad.

The formulation of the remaining two boundary conditions related to the axial force and deformation in the interface is more difficult. The friction force in the interface fuel-clad is indeed a shearing force. But it is treated as a principal axial force in order to apply the formalism valid for axisymmetry and plane strain. For thermal expansion experiments <28> a sliding of the fuel along the sheath was only observed for a rather short fuel length. In analogy the friction force is hypothetically assumed to be such that the fuel and sheath strain in the axial direction are equal. Furthermore the sum of the internal axial forces is equal to the sum of the external axial forces.

$$2 \int_{r_0}^{r_F} \sigma_{Z,F} r dr + 2 \int_{r_F}^{r_{CL}} \sigma_{Z,CL} r dr = r_0^2 P_i - P_o r_{CL}^2 \quad (27)$$

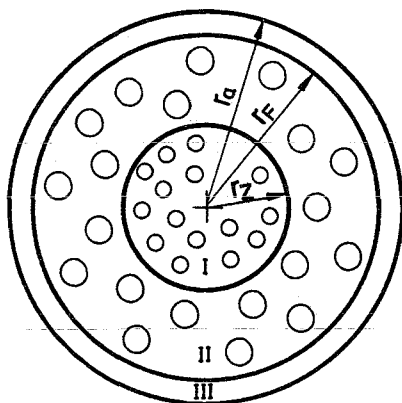
$P_i$  = inner gas pressure

$P_o$  = outer coolant pressure

The other symbols are given by fig. 11

It must be noted, that the swelling is not restrained at the inner fuel radius because of the existence of the central void. Furthermore the central void might be closed like a central void bubble so that its gas pressure could be unequal to that within the plenum.

For the second case of a solid cylindrical fuel the application of a three-zone model according to fig. 12



I = inner fuel zone

II = outer fuel zone

III = cladding

$r_z$  = outside radius of the inner zone

$r_F$  = outside radius of the outer zone

$r_a$  = cladding outside radius

Fig. 12 Three-zone model for the case of a solid cylindrical fuel

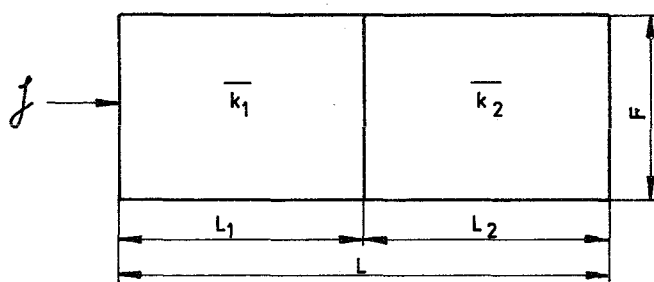
is necessary for the following reasons. The assumptions of a strong friction force between fuel and clad and the condition of plane strain do not allow a movement of any part of the fuel relative to the clad on the base of a two zone model. Because of the rather good creep behavior of the center regions, a relative axial movement has to be allowed. This is possible by the introduction of an inner fuel zone. The axial friction force between the inner and outer fuel zone is assumed to be negligible. It has to be distinguished whether the central core is realized along the total length of the fuel or whether it is restrained axially by fuel because of the inferior creep properties of the cold ends of the fuel. While in the first case the center core exerts no hydrostatic pressure on the outer fuel, a hydrostatic pressure is realized in the case of axial restraint by the fuel. The last case could be realized for solid carbide because of no central void formation for medium linear rod powers.

Appendix

A. Deduction of the porosity dependence of the thermal conductivity

By assuming a stationary heat current without sources flowing parallel or normal through an arrangement of slabs the following relations can be obtained by simple considerations.

The thermal conductivity of the connection in series according to the following figure



$\overline{k}_i$  = (Temperature averaged) thermal conductivity of phase i  
 $L_i$  = length of the phase i  
 $L$  = total length

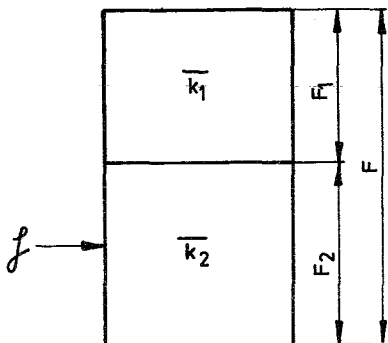
is given by

$$\frac{l}{\overline{k}_s} = \frac{l_1}{\overline{k}_1} + \frac{l_2}{\overline{k}_2} \quad (A1)$$

with  $\overline{k}_s$  = (temperature averaged) thermal conductivity of the connection in series

$$l_i = \frac{L_i}{L}$$

The thermal conductivity of the connection in parallel according to the following figure



$F_i$  = cross sectional area of the phase i  
 $F$  = total cross sectional area

is given by:

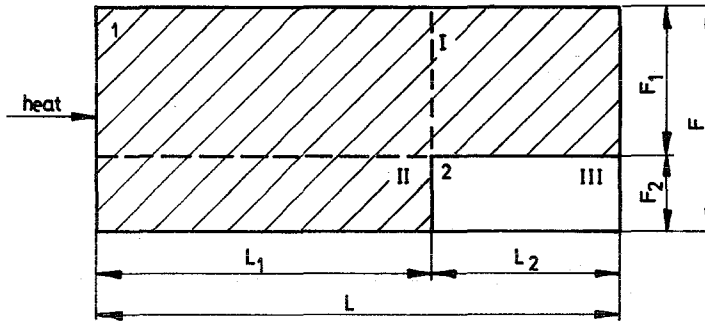
$$\overline{k}_{\text{Par}} = f_1 \overline{k}_1 + f_2 \overline{k}_2 \quad (\text{A2})$$

with

$\overline{k}_{\text{Par}}$  = (temperature averaged) thermal conductivity of the connection  
in parallel

$$f_i = \frac{F_i}{F}$$

In order to use these equations for the calculation of the assumed model



it is necessary to make the volumes sufficiently small. Then the tube of the current can be assumed as a parallelepiped. Furthermore the contribution of the heat produced in the volume to the heat current entering through the cross sectional area F can be neglected. Thus the local thermal conductivity is obtained.

In order to calculate the thermal conductivity of the arrangement above the thermal conductivity for the connection in series of the volume II of phase 1 and the volume III of phase 2 is first calculated with (A1). Then by connecting in parallel this volume with the volume I of phase 1 and by application of

$$l_1 = 1 - l_2 \quad \text{and} \quad f_1 = 1 - f_2 \quad (\text{A3})$$

the following relation is obtained.

$$k = k_1 \left[ 1 - f_2 \left( 1 - \frac{1}{1 + l_2 \left( \frac{k_1}{k_2} - 1 \right)} \right) \right] \quad (\text{A4})$$

In the following  $f_2$  and  $l_2$  are replaced by the relative pore volume fraction P. By the relations:

$$P = \frac{V_2}{V} = \frac{F_2 \cdot L_2}{F \cdot L} = f_2 \cdot l_2 \quad (A5)$$

$$f_2 = \frac{F_2}{F} = \frac{X_2 \cdot Y_2}{X \cdot Y} = x_2 \cdot y_2 \quad (A6)$$

with X, Y,  $X_2$ ,  $Y_2$  as the linear dimensions belonging to F resp.  $F_2$ , and

$$x_2 = a' \cdot l_2 \quad (A7)$$

$$y_2 = a'' \cdot l_2 \quad (A8)$$

with  $a'$  and  $a''$  as anisotropy factors, which must be 1 for the special case of an isotropic pore distribution, the following equations are obtained

$$l_2 = \frac{1}{\sqrt[3]{a' \cdot a''}} P^{1/3} \quad (A9)$$

$$f_2 = \sqrt[3]{a' \cdot a''} P^{2/3} \quad (A10)$$

with  $\sqrt[3]{a' \cdot a''} = a$  and the last two equations the following general porosity dependence of the thermal conductivity finally results:

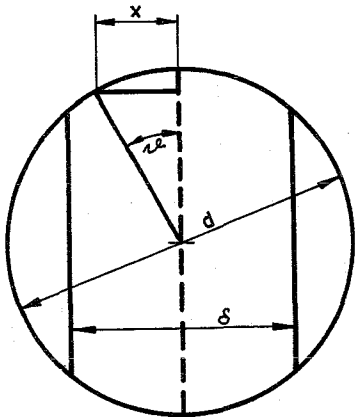
$$k = k_o \left[ 1 - aP^{2/3} \left( 1 - \frac{1}{1 + \frac{1}{a} P^{2/3} \left( \frac{k_o}{k_p} - 1 \right)} \right) \right] \quad (A11)$$

$k_o$  = fully dense phase 1

P = pore phase 2

B. Transformation of the unidimensional gap geometry to the cylindrical and spherical pore geometries relating to the heat transfer by radiation

The transformation is approximately performed by substituting the cylindrical resp. spherical surface of the pore by a plane one as follows.



$$x = \frac{d}{2} \sin \vartheta$$

$d$  = diameter of the cylindrical resp. spherical pore

$\delta$  = equivalent gap width of the unidimensional gap geometry

a. cylindrical pore the axis of which is perpendicular to the heat flow.

$$\frac{\delta}{2} \frac{\pi}{2} = \int_{\vartheta=0}^{\pi/2} x \, d\vartheta$$

$$\delta = \frac{2}{\pi} d = 0.64 d$$

(B1)

b. spherical pore

$$\frac{\delta}{2} 2\pi = \iint_{\text{half sphere}} x \, d\Omega$$

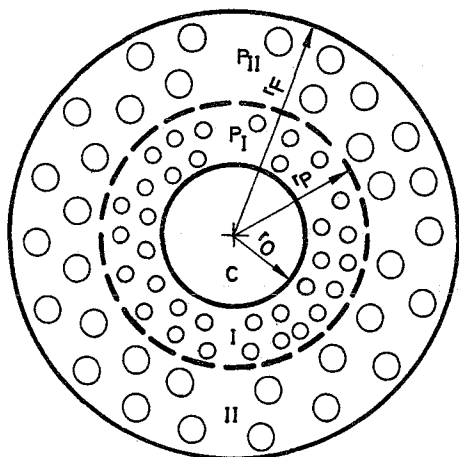
$$\delta = \frac{\pi}{4} d = 0.79 d$$

(B2)

C. Calculation of the thermal central void effect

1. Two - zone porosity model for in-pile porosity migration

The following two - zone porosity model is taken as basis



- C = central void
- I = inner zone of homogenous porosity  $P_I$
- II = outer zone of homogenous porosity  $P_{II}$
- $r_o$  = radius of central void  $T_o = T(r_o)$
- $r_p$  = zone boundary radius  $T_p = T(r_p)$
- $r_F$  = fuel radius  $T_F = T(r_F)$
- T = temperature

Under fast flux conditions the heat source density in each zone is constant. For cylindrical geometry and radial heat flow directed to the outside the following equations for the heat flux density in the two zones result from the heat balance equation

$$\text{zone I: } j(r) = \frac{q_I}{2} \left( r - \frac{r_o^2}{r} \right) \quad (C1)$$

$$\text{zone II: } j(r) = \frac{q_{II}}{2} \left( r - \frac{r_p^2}{r} \right) + j_p \frac{r_p}{r} \quad (C2)$$

$j$  = heat flux density  $\left[ \frac{W}{cm^2} \right]$ ,  $j_p = j(r_p)$   
 $q$  = heat source density  $\left[ \frac{W}{cm^3} \right]$

$j_p$  is given by equation (C1). By means of the Fourier law for cylindrical geometry and radial heat flux

$$j = -k \frac{dT}{dr} \quad (C3)$$

$k$  = thermal conductivity

and the porosity dependences of the thermal conductivities for the two zones according to the  $(1 - P^{2/3})$ -relation

$$k_I(T,P) = k_o(T) (1 - P_I^{2/3}) \quad k_{II}(T,P) = k_o(T) (1 - P_{II}^{2/3}) \quad (C4)$$

$k_o$  = thermal conductivity of the fully dense material

the following equations for the temperature drop in the two zones are obtained

$$\int_{T_P}^{T_o} k_o(T) dT = \frac{q_I}{2(1 - P_I^{2/3})} \left[ \frac{r_P^2 - r_o^2}{2} - r_o^2 \ln \frac{r_P}{r_o} \right] \quad (C5)$$

$$\int_{T_F}^{T_P} k_o(T) dT = \frac{1}{1 - P_{II}^{2/3}} \left[ \frac{q_{II}}{4} (r_F^2 - r_P^2) + \left( \frac{q_I}{2} (r_P^2 - r_o^2) - \frac{q_{II}}{2} r_P^2 \right) \ln \frac{r_F}{r_P} \right] \quad (C6)$$

For comparison the relative fuel density  $D_o$  resp. heat source density  $q_o$  for a solid cylinder of the same linear rod power and the same fuel radius are introduced. As reference also a hollow cylinder with homogenous porosity distribution can be used. Than  $D_o$  means the smear density relating to the fuel radius, the same is valid for  $q_o$ . For fast flux conditions the following relations are valid

$$q_I : q_{II} : q_o = D_I : D_{II} : D_o \quad (C7)$$

with  $D_I = 1 - P_I$  and  $D_{II} = 1 - P_{II}$  (C8)

The linear rod power for the solid and two-zone hollow cylinder is given by

$$\chi = q_o r_F^2 \pi = q_I \pi (r_P^2 - r_o^2) + q_{II} \pi (r_F^2 - r_P^2) \quad (C9)$$

$D$  = relative fuel density

$P$  = porosity

$\chi$  = linear rod power

By eliminating of  $q_I$  and  $q_{II}$  in equation (C5) and (C6) by (C7), (C8) and (C9) the following equations are obtained:

$$\int_{T_P}^{T_O} k_o(T) dT = \frac{\chi}{4\pi D_o} \frac{1 - P_I}{1 - P_I^{2/3}} \left[ \left( \frac{r_P}{r_F} \right)^2 - \left( \frac{r_o}{r_F} \right)^2 - \left( \frac{r_o}{r_F} \right)^2 \ln \left( \frac{r_P}{r_o} \right)^2 \right] \quad (C10)$$

$$\int_{T_F}^{T_P} k_o(T) dT = \frac{\chi}{4\pi D_o} \frac{1 - P_{II}}{1 - P_{II}^{2/3}} \left[ 1 - \left( \frac{r_P}{r_F} \right)^2 + \left( \frac{D_o}{1 - P_{II}} - 1 \right) \ln \left( \frac{r_F}{r_P} \right)^2 \right] \quad (C11)$$

## 2. Homogenous porosity distribution in the hollow cylinder

By substituting  $T_P$  by  $T_F$  and  $r_P$  by  $r_F$  in (C5), doing the same in (C9) and using the temperature averaged thermal conductivity  $\bar{k}_o$  the following relation for the temperature drop in the hollow cylinder is obtained:

$$T_o - T_F = \frac{\chi_H}{4\pi \bar{k}_o (1 - P_H^{2/3})} \left[ 1 - \frac{r_o^2}{r_F^2 - r_o^2} \ln \left( \frac{r_F}{r_o} \right)^2 \right] \quad (C12)$$

$P_H$  = porosity of the hollow cylinder

$r_o$  = radius of the central void

$\bar{k}_o$  = temperature averaged thermal conductivity of the fully dense material

Index H marks the hollow cylinder

The temperature drop in the gap fuel-clad is given by

$$T_F - T_I = \frac{\chi}{2\pi \cdot r_F \cdot h} \quad (C13)$$

$T_I$  = clad inner temperature

$h$  = heat transfer coefficient fuel clad

The total temperature drop in the fuel and gap is given by:

$$(T_o - T_I)_H = \frac{\chi_H}{2\pi} \left[ \frac{1 - \frac{1}{(r_F/r_o)^2 - 1} \ln (r_F/r_o)^2}{2\bar{k}_o (1 - P_H^{2/3})} + \frac{1}{r_F h} \right] \quad (C14)$$

For the solid cylinder the corresponding equation is obtained

$$(T_o - T_I)_S = \frac{\chi_S}{2\pi} \left[ \frac{1}{2\bar{k}_o (1 - P_S^{2/3})} + \frac{1}{r_F h} \right] \quad (C15)$$

$P_S$  = porosity of the solid cylinder. Index S marks the solid cylinder

It is assumed that the smear density  $D_o$  remains constant during the central void formation. By means of the relation

$$D_o = (1 - P_H) \left[ 1 - \left( \frac{r_o}{r_F} \right)^2 \right] = 1 - P_S \quad (C16)$$

finally the following relation for the ratio of the linear rod powers of the hollow and solid cylinder is obtained for the assumption that the total temperature drop  $T_o - T_I$  remains constant

$$\frac{\chi_H}{\chi_S} = \frac{\frac{r_F h}{2\bar{k}_o \left[ 1 - (1 - D_o)^{2/3} \right]^{+1}}}{\frac{r_F h \left[ 1 - \frac{1}{(r_F/r_o)^2 - 1} \ln (r_F/r_o)^2 \right]}{2\bar{k}_o \left[ 1 - \left( 1 - \frac{D_o}{1 - (r_o/r_F)^2} \right)^{2/3} \right]} + 1} \quad (C17)$$

D. Deduction of the equation for the temperature drop in the ideal open gap

By integrating the Fourier law in the unidimensional form

$$j = -k(T) \frac{dT}{dx} \quad (D1)$$

$j$  = heat flux density

$k(T)$  = thermal conductivity of the gas contents within the gap

$\frac{dT}{dx}$  = temperature gradient

over the gap width the following equation is obtained

$$j = \frac{\bar{k}}{\delta} (T_F - T_I) = h (T_F - T_I) \quad (D2)$$

with

$$\bar{k} = \frac{1}{T_F - T_I} \int_{T_I}^{T_F} k(T) dT \quad (D3)$$

$\delta$  = gap width

$h$  = heat transfer coefficient for the gap fuel-clad

$T_F$  = fuel surface temperature

$T_I$  = internal clad temperature

Assuming the thermal conductivity of the filling gas in the following form

$$k = k_C T^s \quad (D4)$$

$k_C, s$  = gas constants

the following equation for the conduction part of the heat transfer is obtained

$$j_C = c_C \frac{1}{\delta} T_I^{s+1} \left[ \left( 1 + \frac{\Delta T}{T_I} \right)^{s+1} - 1 \right] \quad (D5)$$

with

$$c_C = \frac{k_C}{s+1}$$

$\Delta T = T_F - T_I$  = temperature drop in the gap

The total heat flux density given by

$$j_{\text{tot}} = \frac{\chi}{2\pi r_I} = j_C + j_R \quad (\text{D6})$$

is the sum of two components, the conduction part and the radiation part given by the Stefan - Boltzman law

$$j_R = C_R T_I^4 \left[ \left(1 + \frac{\Delta T}{T_I}\right)^4 - 1 \right] \quad (\text{D7})$$

with

$$C_R = \frac{\sigma}{\frac{1}{\epsilon_1} + \frac{1}{\epsilon_2} - 1}$$

$\sigma$  = Stefan - Boltzman constant

$\epsilon_{1,2}$  = emissivities of the fuel resp. the internal clad surface

Solving the equation (D6) with respect to the gap width  $\delta$  the following relationship is obtained

$$\delta = \frac{C_C T_I^{s+1} \left[ \left(1 + \frac{\Delta T}{T_I}\right)^{s+1} - 1 \right]}{\frac{\chi}{2\pi r_I} - C_R T_I^4 \left[ \left(1 + \frac{\Delta T}{T_I}\right)^4 - 1 \right]} \quad (\text{D8})$$

From (D5), (D6), (D7) and (D2) results for  $\Delta T \ll T_I$  the following expression for the heat transfer coefficient  $h$

$$h = \frac{\bar{k}_G}{\delta} = k_C T_I^s \frac{1}{\delta} + 4C_R T_I^3 \quad \Delta T \ll T_I \quad (\text{D9})$$

where  $k_C$  = (temperature averaged) "thermal conductivity of the gap".

Literature:

- ⟨1⟩ J. Vogt, L. Grandell and M. Rumfors, AB Atomenergi (Sweden) Int. Report RBM - 527 (1964) cited by IAEA Pael on Thermal Conductivity in Uranium Dioxide, Vienna 1966, Techn. Report Series No. 59
- ⟨2⟩ M.J.F. Notley and J.R. Mac Ewan, Nucl. Appl. 2, 117, (1966)
- ⟨3⟩ A.M. Ross "The Dependence of the Thermal Conductivity of Uranium Dioxide on Density, Microstructure, Stoichiometry and Thermal Neutron Irradiation" AEC1 - 1096 (1960)
- ⟨4⟩ J.A.L. Robertson, A.M. Ross, M.J.F. Notley and J.R. Mac Ewan "Temperature Distribution in UO<sub>2</sub> Fuel Elements". J. Nucl. Mat. 7, No. 3 (1965)
- ⟨5⟩ H. Mogard, S. Djurle, I. Multer, H.P. Meyers, B. Nelson and M. Rumfors "Fuel Development for Swedish Water Reactors", Geneva Conference P/608 (1964)
- ⟨6⟩ M.J.F. Notley and J.R. Mac Ewan "The Effect of UO<sub>2</sub> Density on Fission Product Gas Release and Sheath Expansion" AEC1 - 2230 (1965)
- ⟨7⟩ R.R. Asamoto, F.L. Anselin and A.E. Conti "The Effect of Density on the Thermal Conductivity of Uranium Dioxide." J. of Nuc. Mat. 29, 67 (1969)
- ⟨8⟩ A.L. Loeb, "A Theory of Thermal Conductivity of Porous Materials" J. Am. Ceram. Soc. 37, No.2, 96, (1954)
- ⟨9⟩ A. Eucken "Die Wärmeleitfähigkeit keramischer feuerfester Stoffe" VDI - Forschungsheft 353/ April 1932
- ⟨10⟩ H.W. Russell "Principles of Heat Flow in Porous Insulators" J. Am. Ceram. Soc. 18, 1, (1955)
- ⟨11⟩ A. Biancheria, "The Effect of Porosity on Thermal Conductivity of Ceramic Bodies". Trans. ANS 9, No. 1, 15 (1966)
- ⟨12⟩ A. Biancheria, "The Thermal Conductivity of Multiphase Ceramic Nuclear Fuels" Trans. ANS 10, 1, 100, (1967)
- ⟨13⟩ C.W. Sayles "A Three-Region Analytical Model for the Description of the Thermal Behaviour of Low-Density Oxide Fuel Rods in a Fast Reactor Environment" Trans. ANS 10, 2, 458, (1967)

- <14> E.G. Stevens "Derivation of a Sintering Correction Factor for Fast Oxide Fuels" Trans. ANS 11, 1, 130 (1968)
- <15> E.G. Stevens "A Correction Factor for in-Reactor Sintering of Fast Oxide Fuels". Nucl. Appl. 5, 410, (Dec. 1968)
- <16> H. Kämpf "The Influence of Inner Geometry on Temperature Distribution of Fast reactor Fuel Pins" KFK 751 - EUR 3710 d (Febr. 1968) (in German)
- <17> J.A. Christensen "Uranium Dioxide Thermal Conductivity" - Trans. ANS 7, 2 - (1964)
- <18> J. Hetzler, E. Zebroski "Thermal Conductivity of Stoichiometric and Hypo-stoichiometric Uranium Oxide at High Temperatures" Trans. ANS 7, 2, 392 (1964)
- <19> D.M. Coplin et.al. "In-pile Direct Measurement of  $UO_2$  Thermal Conductivity" Trans. ANS 8, 1, 35 (1968)
- <20> W.E. Bailey et. al. " In-Pile Thermal Conductivity of  $UO_2$  and 20/80 (Pu/U) $O_2$  Specimens" Trans. ANS 8, 1, 39 (1965)
- <21> J. Hetzler et. al. "Thermal Conductivity of 20/80(Pu/U) $O_2$ " - Trans- ANS 8, 1, 36 (1965)
- <22> H.E. Schmidt, Tu-Karlsruhe, unpublished
- <23> H. Kämpf "General gap equation for the heat transfer through the gap fuel-clad in fuel elements with pellet fuel" KFK 604 (June 1967) (in German)
- <24> H. von Ubisch, S. Hall and R. Srivastov "Thermal Conductivities of Mixtures of Fission Product Gases with Helium and Argon" 2nd United Nations Intern. Conf. on the Peaceful Uses of Atomic Energy A/Conf. 15/P/143, Sweden, (1958)
- <25> G.V. Massey "The Thermal Properties of Gases for Use in Reactor Heat - Transfer Calculations" DEG - Report 14(P), 1960

- ⟨26⟩ M. Guyette "Crash: A Computer Programme for the Analysis of Creep and Plasticity in fuel pin sheaths", KFK 1050 (August 1969)
- ⟨27⟩ B. Wedell " A Theoretical Evaluation of Crack Formation in  $UO_2$ -Fuel Pellets and its Effect upon DOR - Reactor Fuel Element design". Risö Report No. 52 (July 1962)
- ⟨28⟩ M.J.F. Notley, A.S. Bain and I.A.L. Robertson "The Longitudinal and Diametral Expansions of  $UO_2$  Fuel Elements". AEC1 - 2143 (Nov. 1964)
- ⟨29⟩ H. Marchandise " Dilation Thermique du Bioxide d'Uranium en Pile, Essai de Synthese", EUR 4033f, (1968)
- ⟨30⟩ H. Kämpf, "Carbide Fuels for fast breeder reactors - Contribution XI: The possibilities of a fuel pin design". KFK 1111 (1969) (in German)
- ⟨31⟩ R.S. Barnes, R.S. Nelson "Theories of Swelling and Gas Retention in Reactor Materials" AERE - R 4952, (June 1969)
- ⟨32⟩ F.A. Nelson "Behavior of gaseous Fission Products in Oxide Fuel Elements" WAPD - TM - 570 (October 1966)
- ⟨33⟩ J.W. Harrison " The Growth of Gas Bubbles in a Stressed Medium and the Application to Stress Enhanced Swelling in Alpha Uranium " J.N. Mat. 23, 139, (1967)
- ⟨34⟩ V. M. Agranowich "Theory of Fissile Materials Swelling" A/Conf. 28/P/338a (May 1964)

Fig.3: Thermal conductivity as a function of porosity for isotropic pore distribution.

$$\frac{k}{k_0} = 1 - P^{2/3} \left( 1 - \frac{1}{1 + P^{1/3}(\alpha - 1)} \right) \quad \alpha = \frac{k_0}{k_p}$$

$$\alpha \rightarrow \infty \quad \frac{k}{k_0} = 1 - P^{2/3}$$

Linear graph:  $\frac{k}{k_0} = 1 - \eta P$

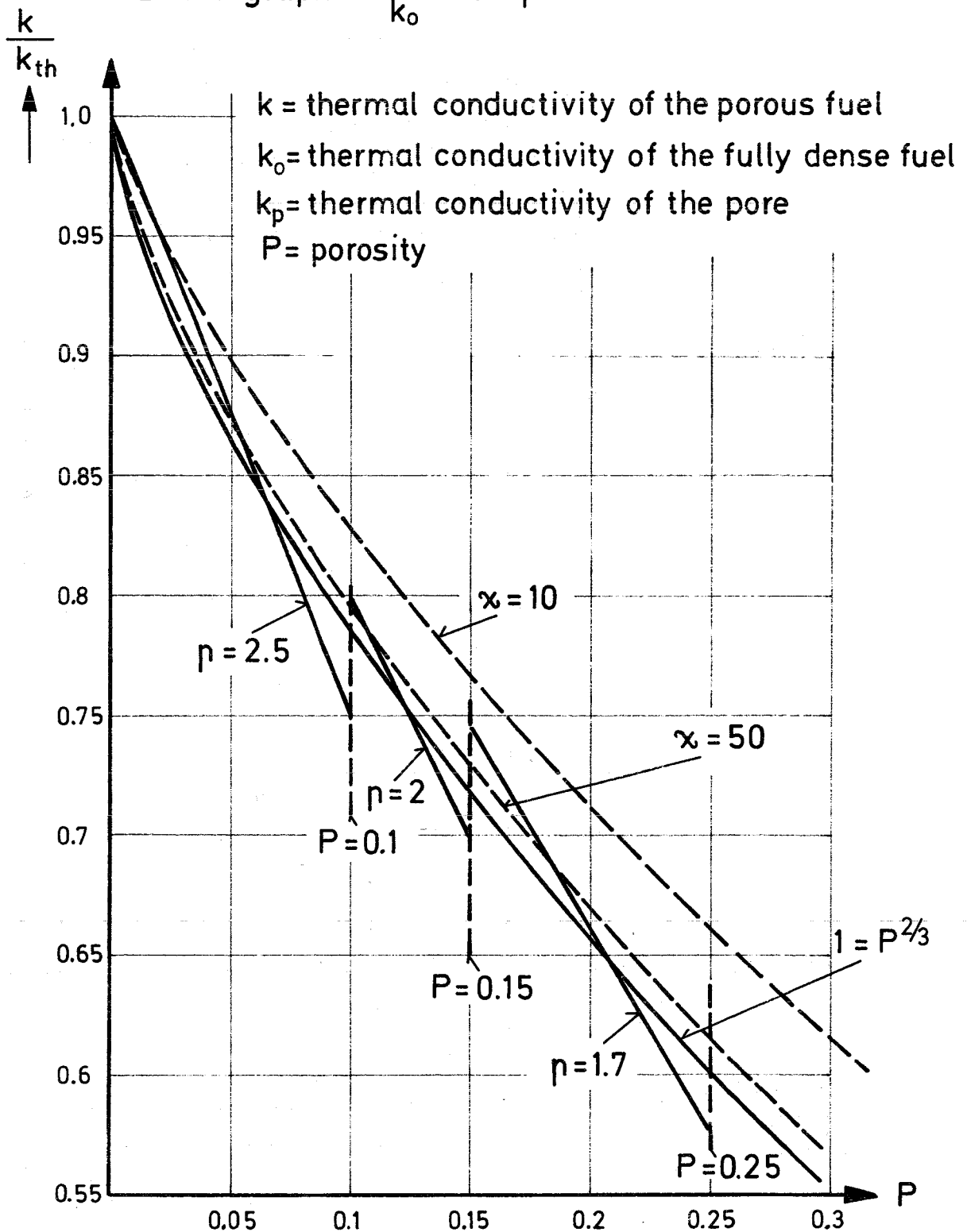


Fig.4: Dependence of the ratio  $\alpha = k_o/k_p$  on pore dimension  $d$  for oxide fuel.

Assumptions:

$$k_{He} = 1.58 \cdot 10^{-5} T^{0.79}$$

$$k_{FP} = 0.77 \cdot 10^{-6} T^{0.79}$$

$$k_{UO_2,0}(1300^\circ K) = 3.33 \cdot 10^{-2}$$

$$k_{UO_2,0}(2000^\circ K) = 2.55 \cdot 10^{-2}$$

$$\frac{W}{cm^\circ C}$$

$$\epsilon = 0.8$$

$$\beta = 0.79 \text{ (spherical pores)}$$

$k_o$  = thermal conductivity of the fully dense  $UO_2$

$k_p$  = thermal conductivity of the pore

$k_i$  = thermal conductivity of the filling gas  
 $i = He, FP$  (fission product gas 15% Kr + 85% Xe)

$\epsilon$  = emissivity of the pore surface

$\beta$  = shape factor

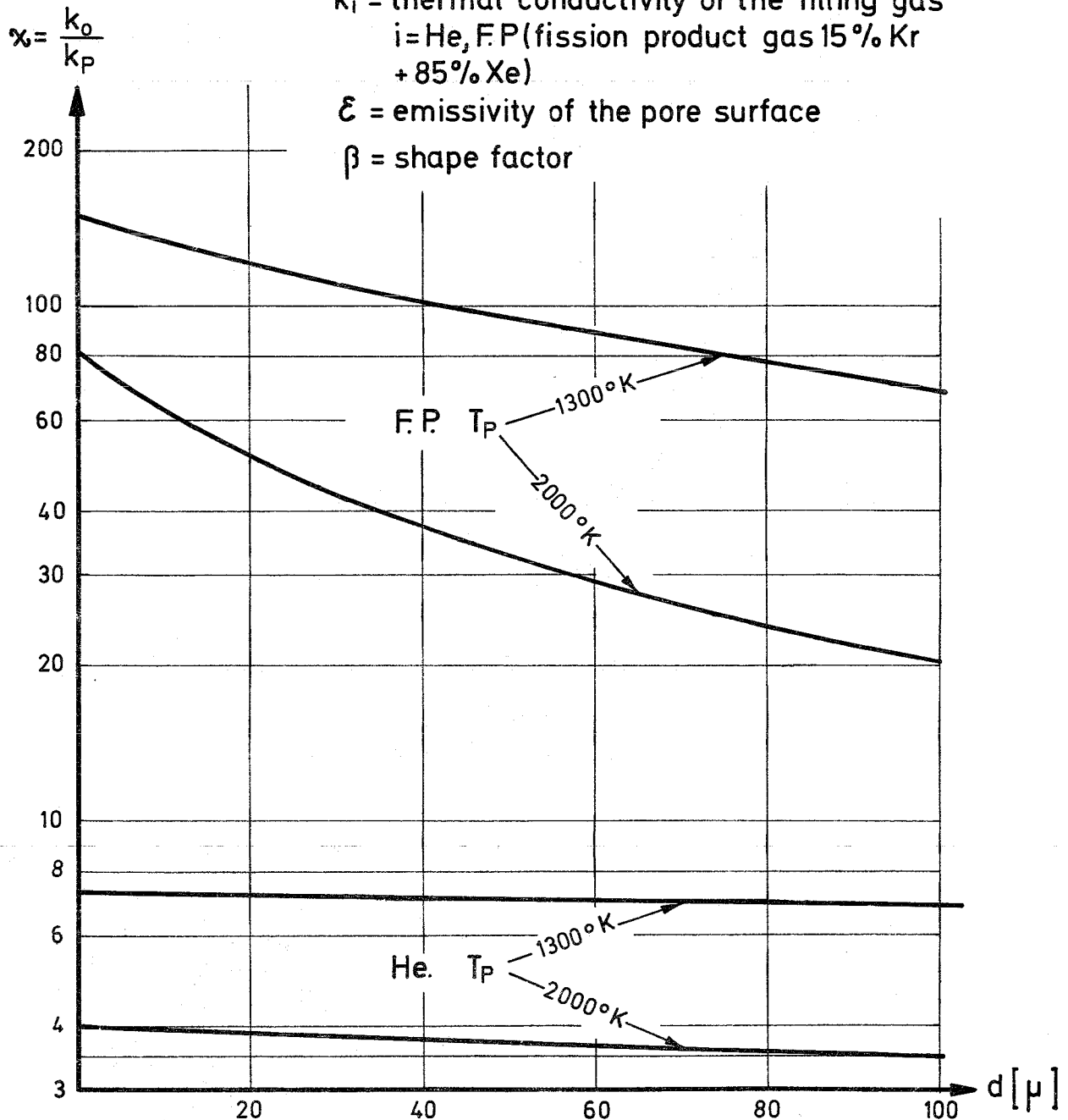


**Fig.6:** Increase of linear rod power by central void formation for homogenous porosity distribution and for in pile porosity migration.

(Central temperature  $T_0$  and clad inner temperature  $T_j$  are constant, smear density  $D_0$  related to fuel radius  $r_F$  is parameter)

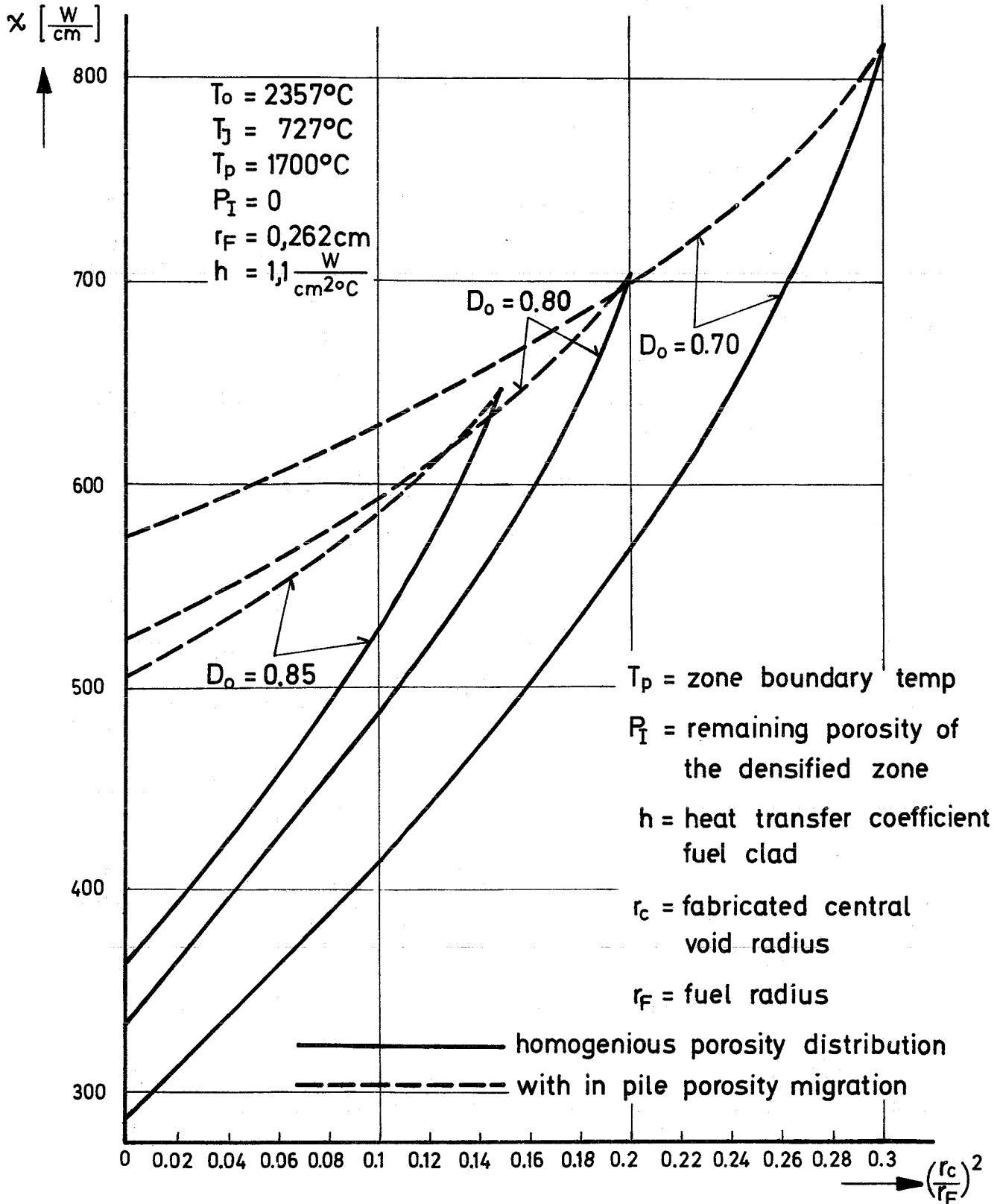


Fig.7: Relative increase of linear rod power by central void formation for oxide and carbide

Assumptions: Homogenous porosity distribution. Central temperature and clad inner temperature are constant.

————— oxide  
 - - - - - carbide

Na-bonding  
 He-bonding

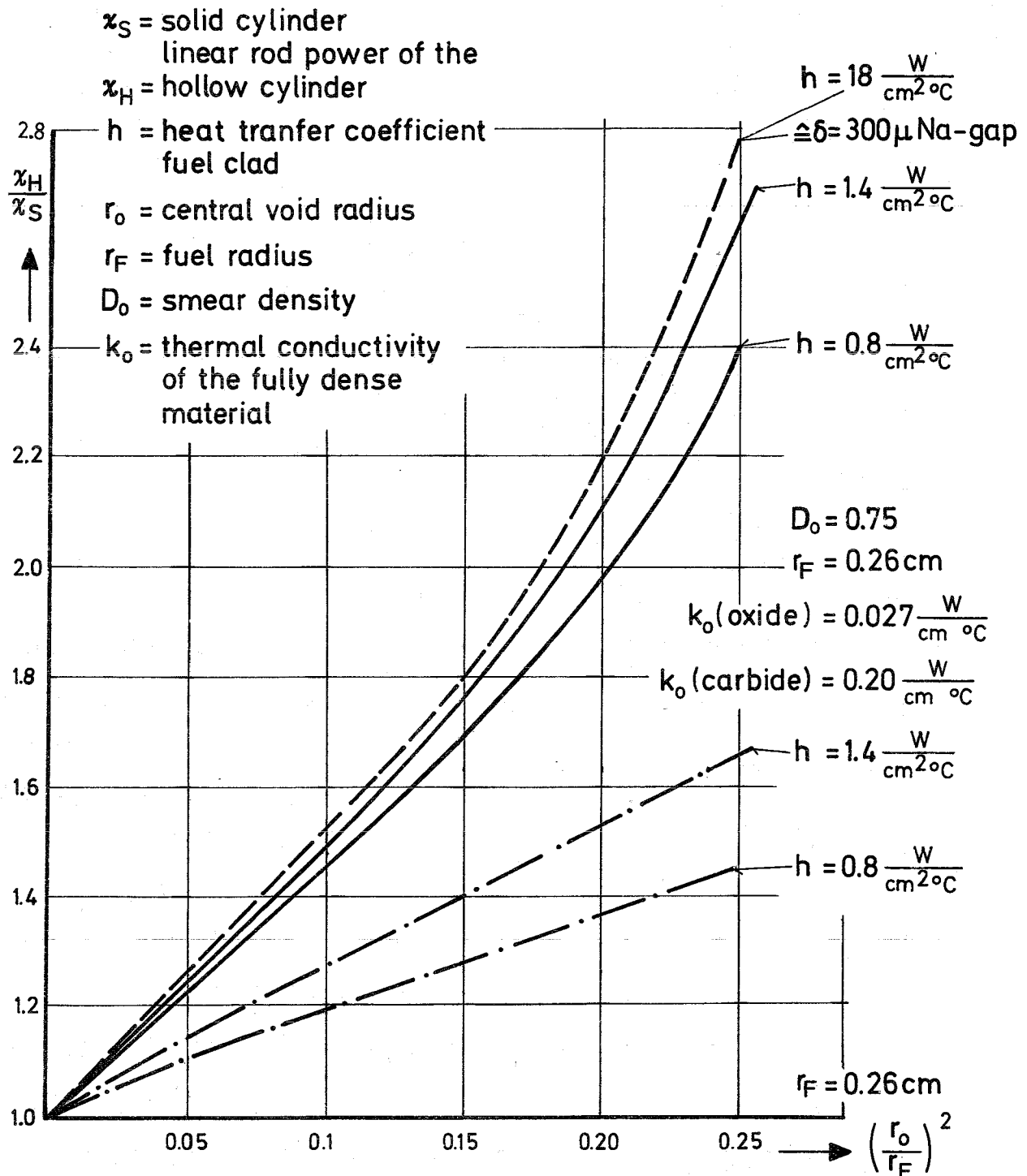
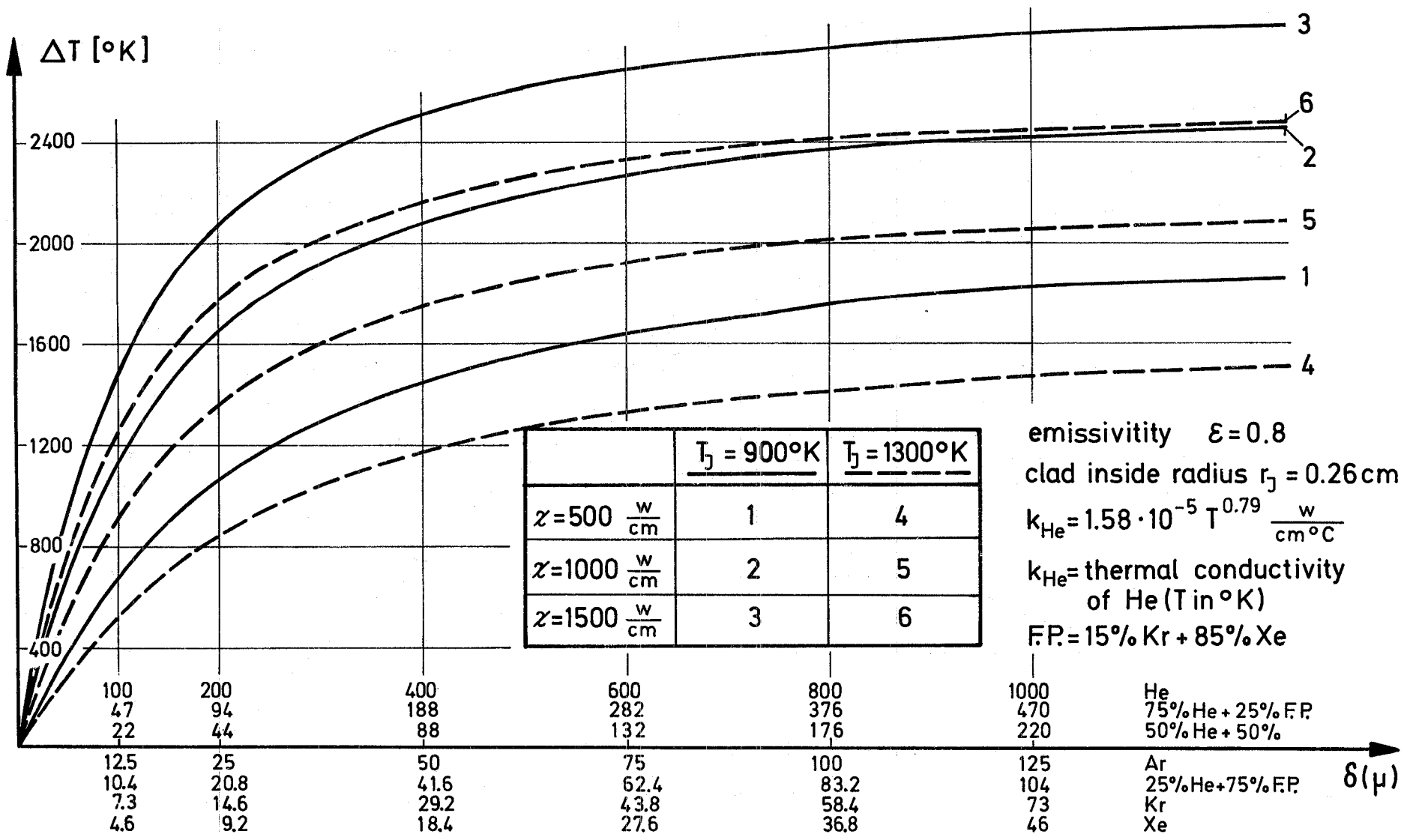
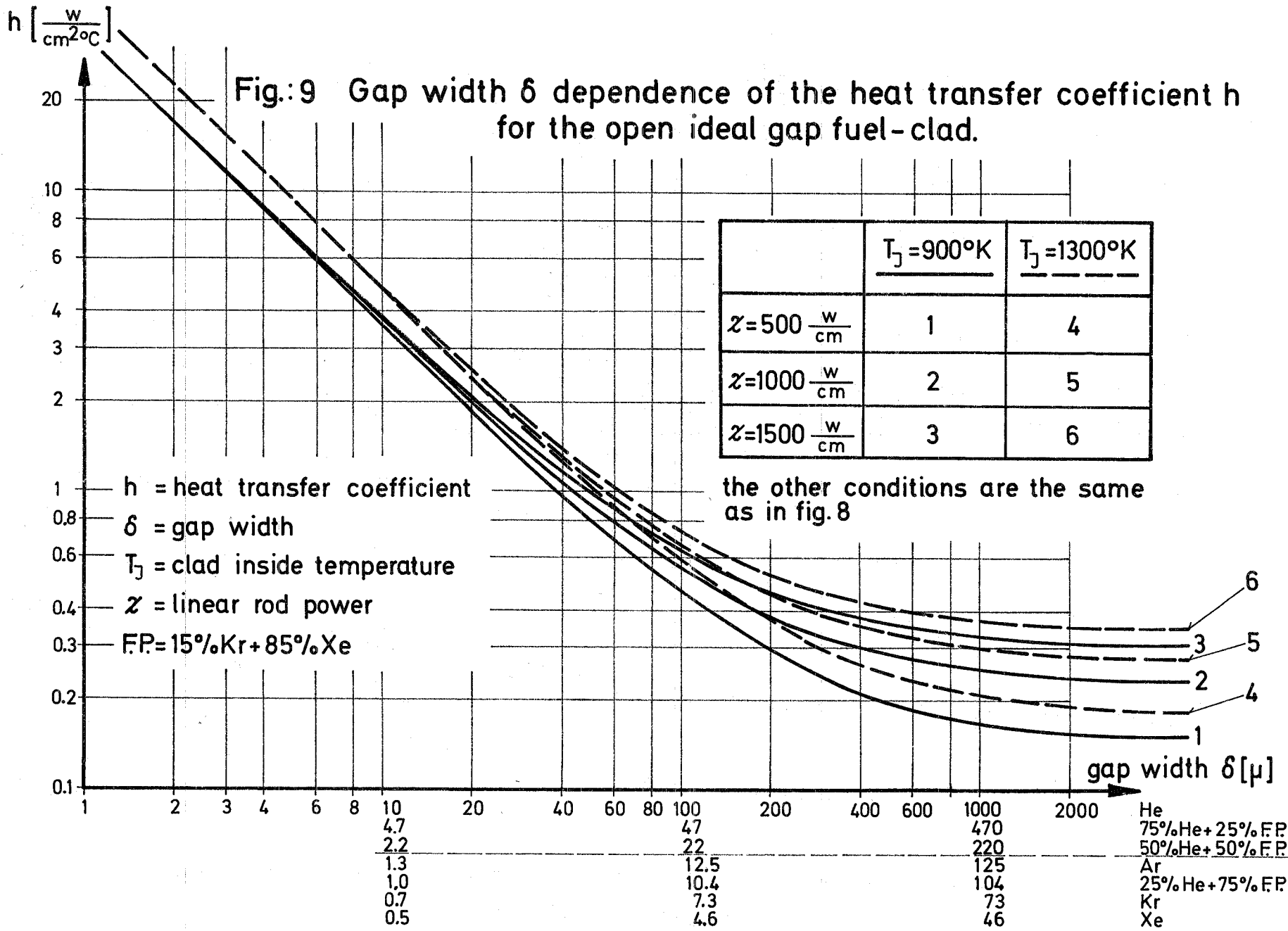


Fig.: 8 Temperature drop  $\Delta T$  as a function of the gap width  $\delta$  for the open ideal gap fuel-clad.

Linear rod power  $\chi$ , clad inside temperature  $T_j$  and gas type are parameter





# Fig.13: Computer listing of the maximum operation times of the Na2-Core

